

Original Research

# Spatial Variability of CO<sub>2</sub>, CH<sub>4</sub>, and N<sub>2</sub>O Fluxes during Midsummer in the Steppe of Northern China

Jianzhong Cheng<sup>1</sup>, Xinqing Lee<sup>1\*</sup>, Benny K.G. Theng<sup>2</sup>, Bin Fang<sup>1,3</sup>,  
Fang Yang<sup>1,3</sup>, Bing Wang<sup>1</sup>, Like Zhang<sup>1,3</sup>

<sup>1</sup>State Key Laboratory of Environmental Geochemistry, Institute of Geochemistry, Chinese Academy of Sciences, Guiyang 550002, PR China

<sup>2</sup>Landcare Research Private Bag 11052, Palmerston North 4442, New Zealand

<sup>3</sup>Graduate University of Chinese Academy of Sciences, 100049, Beijing, PR China

Received: 29 March 2013

Accepted: 25 September 2013

## Abstract

Spatial variability is a major source of uncertainty in estimating the fluxes of greenhouse gases between steppe and atmosphere. The fluxes of CO<sub>2</sub>, CH<sub>4</sub>, and N<sub>2</sub>O were carried out between 08:00 and 10:00 h. of the following day during the midsummer period from a transect (area: 5.25×10<sup>6</sup> ha) in the semiarid steppe of northern China, using the dark static chamber technique and gas chromatography. Two land uses were chosen for this study: soils with plant covers and bare soils. Daily average GHG fluxes from the steppe transect were: 1.3×10<sup>5</sup> t C for CO<sub>2</sub>, -66.3 t C for CH<sub>4</sub>, and 1.1 t N for N<sub>2</sub>O. The emission of CO<sub>2</sub> from soils with plant cover was significantly higher ( $P < 0.05$ ) than that from the corresponding bare soils. The canopy effect, however, was observed for neither CH<sub>4</sub> ( $P = 0.058$ ) nor N<sub>2</sub>O ( $P = 0.772$ ). Air temperature and relative humidity were the major factors affecting the diurnal variation in site-based CO<sub>2</sub> flux ( $P < 0.05$ ), while soil pH controlled its spatial variation ( $P < 0.05$ ). The spatial uptake of CH<sub>4</sub> correlated negatively with soil total N (TN) content ( $P < 0.05$ ), while the flux of N<sub>2</sub>O significantly increased with soil organic carbon ( $P = 0.031$ ) and TN ( $P = 0.022$ ), indicating that soil organic matter is an important factor determining the N<sub>2</sub>O flux in the steppe of northern China.

**Keywords:** carbon cycle, greenhouse gas, climate change, grassland, semiarid region

## Introduction

Carbon dioxide (CO<sub>2</sub>), methane (CH<sub>4</sub>), and nitrous oxide (N<sub>2</sub>O) are major greenhouse gases (GHG) in the atmosphere and significant contributors to global warming. Soils are important sources and sinks of CO<sub>2</sub>, CH<sub>4</sub>, and N<sub>2</sub>O. Since the emission of these gases from soil is a microbially induced process, the variation in flux is influenced by soil temperature, moisture, O<sub>2</sub> concentration, fertilizers, and

organic substrate decomposition as well as C and N availability [1, 2]. GHG fluxes show large spatial variability even in terrestrial ecosystems that appear to be homogeneous [3-6]. As a result, there is much uncertainty in estimating the flux of GHG between terrestrial ecosystem and atmosphere.

Grasslands make up about 25% of the Earth's terrestrial ecosystem [7] and hold 10-30% of the global soil carbon stocks [8, 9]. The exchange of CO<sub>2</sub>, CH<sub>4</sub>, and N<sub>2</sub>O between grassland and atmosphere would, therefore, have a significant impact on atmospheric GHG concentrations and the

---

\*e-mail: lee@mail.gyig.ac.cn

Table 1. Location and characteristics of sampling sites.

Symbol	Site name	Plant types	Soil type	Alt. (m)	Long. (E)	Lat. (N)	Date (mm/dd/yyyy)
A	Etuoke Banner	<i>Stipa bungeana</i> (St)	Castanozems	1286	107.36	38.86	08/20/2010
B	Otog Front Banner – A	<i>Peganum harmala</i> (Ph); <i>Stipa bungeana</i> (Sb)	Castanozems	1425	107.23	38.49	08/22/2010
C	Otog Front Banner – B	<i>Sophora alopecuroides</i> (Sa)	Aeolian soil	1328	107.56	38.36	08/25/2010
D	Yanchi	<i>Artemisia scoparia</i> (As)	Cinnamon soil	1370	106.76	37.53	08/28/2010
E	Tongxin-A	<i>Peganum harmala</i> ; <i>Stipa bungeana</i>	Cinnamon soil	1362	106.49	37.34	08/30/2010
F	Tongxin-B	<i>Artemisia scoparia</i>	Cinnamon soil	1636	106.01	37.10	08/31/2010
G	Haiyuan	<i>Artemisia scoparia</i> ; <i>Pennisetum centrasiatium</i> (Pc)	Loess	1728	105.87	36.46	09/04/2010
H	Guyuan	<i>Pennisetum centrasiatium</i>	Loess	1719	106.23	36.02	09/07/2010

Letters in brackets indicate the abbreviation of plant types.

biogeochemical cycling of C and N. Natural grasslands constitute ca  $3.9 \times 10^8$  ha of China's territory, accounting for about 41% of the total national land area and nearly 12.5% of the world's area. The semiarid steppe in northern China accounts for about 78% of the total grassland area in the country [10]. Recently, climate change has led to rapid loss of soil organic carbon (SOC) in the northern Chinese steppe [11], which, in turn, may exert a significant effect on the GHG budget in the semiarid region.

Previous studies have indicated that spatial patterns in GHG fluxes at a relatively large scale are found to be complicated [3, 4, 6, 12, 13].  $\text{CO}_2$  fluxes from soils have high spatial heterogeneities [4, 12], which is a problem in precisely estimating  $\text{CO}_2$  fluxes over large areas.  $\text{CH}_4$  and  $\text{N}_2\text{O}$  fluxes also show large spatial variability [3, 4, 13]. Besides such large inconsistent spatial heterogeneities, GHG fluxes have been found to vary relationships with environmental factors. Working in the Xilin river catchment, Yao et al. [5] found that the spatial variability in  $\text{N}_2\text{O}$  and  $\text{CO}_2$  emissions was primarily influenced by soil moisture, while in the Qinghai-Tibetan Plateau the flux of  $\text{CH}_4$  and  $\text{N}_2\text{O}$  was negatively correlated with soil pH [6]. Similarly, soil moisture primarily controls the spatial variability of  $\text{N}_2\text{O}$  emissions in the semiarid grasslands, but soil temperature is the primary influencing factor for  $\text{CH}_4$  uptake [14, 15]. On the other hand, Du et al. [16] did not find a linear relationship between soil moisture and  $\text{N}_2\text{O}$  flux, or between  $\text{N}_2\text{O}$  flux and soil temperature for semiarid grassland soils. This apparent inconsistency may be ascribed to the paucity of data as well as to the introduction of considerable errors when the results were extrapolated to large areas. Thus, the high spatial variability of GHG fluxes, related to influencing factors, requires further research using field measurements over a large scale and across a variety of plant communities [6]. Here we measure the flux of GHG from soils with different plant covers in the semiarid steppe of northern China in order to:

(1) understand its spatial variability

- (2) explain the effect of vegetative cover and type on GHG fluxes
- (3) determine the major factors affecting GHG emission fluxes

## Materials and Methods

### Site Description

During the midsummer period from August 20 to September 7, of 2010, we measured the flux of greenhouse gases ( $\text{CO}_2$ ,  $\text{CH}_4$ , and  $\text{N}_2\text{O}$ ) in soils along a transect from southern Inner Mongolia to the whole of Ningxia province (SIMWN); that is, from latitude  $36^\circ 07' - 38^\circ 52' \text{ N}$  to longitude  $106^\circ 14' - 107^\circ 21' \text{ E}$ . The SIMWN transect is located in the semiarid steppe, comprising the pastoral area of Etuoke Banner and Otog Front Banner in Inner Mongolia, and the agro-pastoral ecotone in the Ningxia Hui Autonomous Region. We selected sampling sites in the vicinity of Etuoke Banner, Otog Front Banner, Yanchi, Tongxin, Haiyuan, and Guyuan, denoted by the symbols A to H (Fig. 1, Table 1). The total length of the sampling transect is about 400 km, and each of the plots selected was some distance away from roads, towns, and villages so as to minimize anthropogenic disturbance and influence.

The dominant regional climate is a temperate semiarid continental monsoon, with a short, variable frost-free growing season. The long-term annual air temperature ranges from 6.2 to 9.0°C with a mean of 7.4°C, a mean maximum of 21.5°C in July, and a mean minimum of -8.7°C in January. The average annual precipitation in the region varies from 220.4 to 439.0 mm, with a multi-year mean of 296.9 mm. Thus, less than 400 mm of annual precipitation is recorded in all of the sampling sites except for the site near Guyuan city. Data provided by meteorological stations along the transect indicate that the annual precipitation is unevenly distributed, with more than 60% of the rainfall falling in the July-September period. The dominant plant

communities at the measurement sites are *Stipa bungeana*, *Peganum harmala*, *Artemisia scoparia*, *Pennisetum centasiaticum*, and *Sophora alopecuroides*. Each community has fewer than 10 common species, and the plants are generally shorter than 50 cm. The soil types along the SIMWN transect comprise Cinnamon soils, Castanozems, Aeolian soils, and Loess (Fig. 1). The location, altitude, latitude, longitude, and sampling date for each site along the transect are given in Table 1.

### Experimental Design

At each sampling site, fluxes of CO<sub>2</sub>, CH<sub>4</sub>, and N<sub>2</sub>O were determined for the bare soil and the corresponding soil covered with 15-30 cm high plants. Measurements were normally carried out from 08:00 h to 10:00 h. of the following day. One set of measurements were done every two hours, using the static black chamber method.

Individual chambers consisted of a fixed stainless steel base (30 cm×30 cm×10 cm) with a U-shaped groove at the top edge, lined with a moveable opaque polyvinyl chloride (PVC) sheet (volume: 0.045 m<sup>3</sup>; 30 cm×30 cm×50 cm).

Once the cover was placed over the base, the groove was filled with water, acting as an air seal. At 0, 5, 10, 15, and 20 minutes after the groove was sealed, a 30 mL air sample was taken from the chamber and then injected into a 12 mL glass bottle that was vacuum-sealed with a butyl rubber stopper and a plastic cap.

The concentrations of GHG were determined using an Agilent 7890 gas chromatograph (GC) equipped with an automatic injector (Gilson 223), an electron capture detector (ECD) for N<sub>2</sub>O, and a flame-ionization detector (FID) for both CH<sub>4</sub> and CO<sub>2</sub> after reduction of the latter gas over a nickel catalyst. More details of the analytical procedure and methods for calculating GHG fluxes have been given by Wang and Wang [17]. Negative flux values indicate uptake by soil of GHG (from the atmosphere), and positive values represent GHG emissions from soil to atmosphere.

### Calculation of Global Warming Potential (GWP)

The GWP of each gas is defined in relation to a given weight of CO<sub>2</sub> for a specified time period. According to the

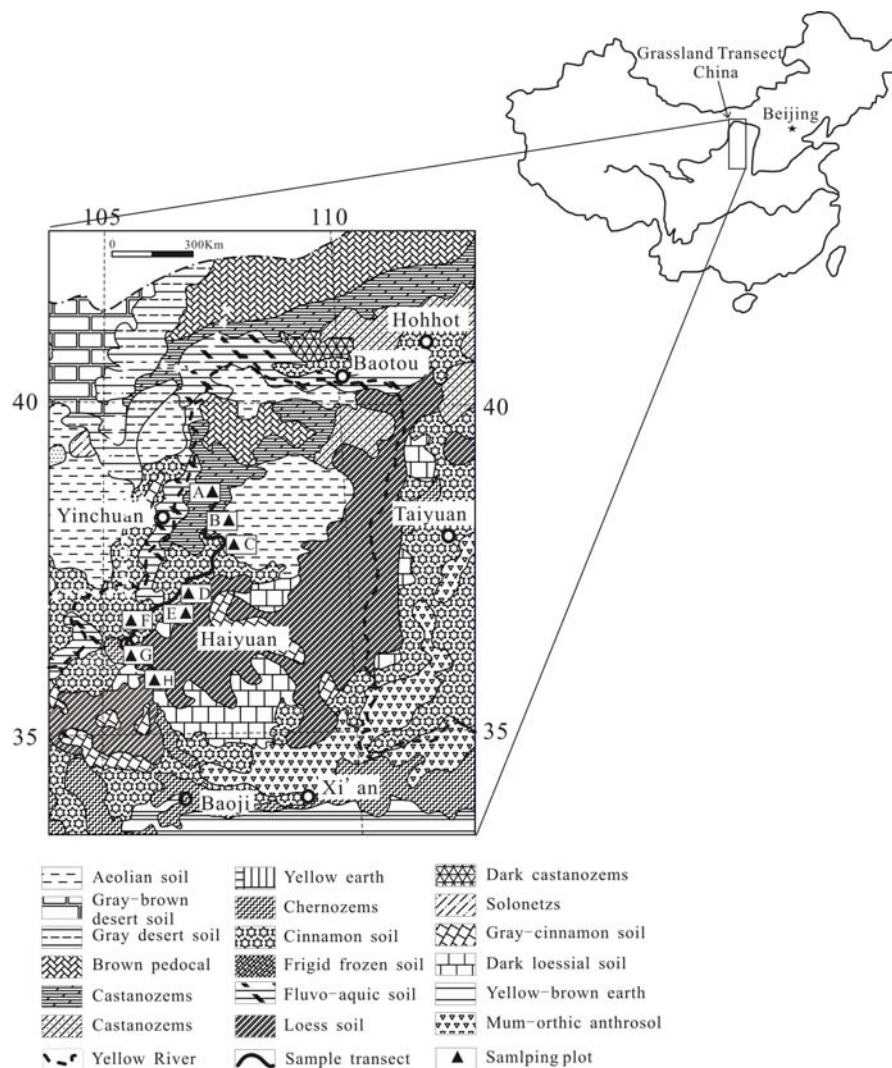


Fig. 1. Location of study sites along a transect from southern Inner Mongolia to the whole of Ningxia province (SIMWN) in northern China.

Table 2. Daily average, minimum, and maximum fluxes of CO<sub>2</sub>, CH<sub>4</sub>, and N<sub>2</sub>O from bare soils and from soils with plant cover along the SIMWN transect.

Fluxes	Bare soil			Plant cover		
	Mean	Min.	Max.	Mean	Min.	Max.
CO <sub>2</sub> flux (mg C m <sup>-2</sup> ·h <sup>-1</sup> )	40.3±16.8	13.0±6.8	68.3±28.3	132.7±56.6	43.7±24.2	344.7±183.7
CH <sub>4</sub> flux (µg C m <sup>-2</sup> ·h <sup>-1</sup> )	-37.0 ±16.2	-67.4 ±19.1	-6.9±9.2	-59.3 ±17.7	-150.5±11.6	-26.5±15.4
N <sub>2</sub> O flux (µg N m <sup>-2</sup> ·h <sup>-1</sup> )	2.2±9.7	-2.9±11.6	6.1±5.4	0.3±8.8	-3.1±6.3	5.9±9.4

Numbers represent measured value±standard deviation

fourth Intergovernmental Panel on Climate Change (IPCC) report, the average GWP for CO<sub>2</sub>, CH<sub>4</sub>, and N<sub>2</sub>O are 1, 25, and 298 at a 100 year time horizon, respectively. Using the IPCC definition, the diurnal GWP may be derived from the following equation:

$$\text{GWP} = \text{FCO}_2 + \text{FCH}_4 \times \text{RFCH}_4 + \text{FN}_2\text{O} \times \text{RFN}_2\text{O} \quad (1)$$

...where FCO<sub>2</sub>, FCH<sub>4</sub>, and FN<sub>2</sub>O are the diurnal fluxes of CO<sub>2</sub>, CH<sub>4</sub>, and N<sub>2</sub>O between grassland ecosystems and the atmosphere, respectively; RFCH<sub>4</sub> and RFN<sub>2</sub>O are constants indicating radiative forcing of CH<sub>4</sub> and N<sub>2</sub>O in terms of a CO<sub>2</sub> equivalent unit, being 25 and 298, respectively, at a 100-year time horizon [18].

### Soil Property Measurements

Soil samples (0-10 cm) were collected from each sampling site at the time of gas flux measurement. The soils were crushed, passed through a 100-mesh sieve, and air-dried. The C and N contents of the soils (and plant tissues) were determined using an elemental analyzer (Model: PE 2400II, Perkin Elmer, USA). Soil NH<sub>4</sub><sup>+</sup>-N contents were determined by extracting the soils with a 2 M KCl solution (1:5 soil to KCl solution), shaking the suspension for 1 hour, filtering through a Whatman #42 filter paper, and analyzing the filtrate with a UV-VIS spectrophotometer. Soil pH was measured in 1:2.5 soil/water solution using a pH meter with a glass electrode. Gravimetric water contents were measured by drying the samples at 105°C for 24 h (to constant weight).

### Statistical Analyses

Differences and standard deviation in CO<sub>2</sub>, CH<sub>4</sub>, and N<sub>2</sub>O fluxes between soil/plant system and atmosphere were analyzed using a one-way ANOVA method followed by the least significant differences (LSD) test. Linear regression models were used to examine the relationships between CO<sub>2</sub>, CH<sub>4</sub>, and N<sub>2</sub>O fluxes, soil/plant properties, and environmental variables, including air temperature, relative humidity (RH), soil pH, NH<sub>4</sub><sup>+</sup>-N, soil organic carbon (SOC), soil total nitrogen (TN), and total plant C and N contents.

Multiple regression analysis was also used to assess the relationship between spatial N<sub>2</sub>O fluxes and SOC as well as TN. All statistical analyses, based on a significance level of P < 0.05, were conducted using the SPSS 13.0 software package (SPSS Inc., Chicago, USA).

## Results

### Carbon Dioxide

Fig. 2 shows the variations in soil CO<sub>2</sub> emission and air temperature during a representative day for eight sites (A to H) along the SIMWN transect (Fig. 1, Table 1). With the exception of plot A, the diurnal variations in CO<sub>2</sub> emissions closely follow those of air temperature, accounting for 44.4-95.6% of the temporal variance in emissions (P < 0.05). Plot A received rain during the night, influencing CO<sub>2</sub> emissions from this site. A significant negative relationship was also observed between diurnal variations in CO<sub>2</sub> fluxes and relative humidity (RH), except for plot A as RH correlated negatively with air temperature across all sites (R<sup>2</sup> = 0.56-0.88, P < 0.05). Soil CO<sub>2</sub> emissions from all plots showed a similar daily variation, with a minimum flux being measured between 05:00 and 06:00 h, and a maximum flux between 11:00 and 14:00 h. The minimum and maximum values of air temperature and RH were recorded for the same time intervals. The flux of CO<sub>2</sub> emissions, measured between 08:00 and 10:00 h, was close to the daily average value (Fig. 2).

The CO<sub>2</sub> flux from bare soils at all sites along the transect ranged from 13.0 to 68.3 mg C m<sup>-2</sup>·h<sup>-1</sup>, while the flux from soils with plant cover ranged from 43.7 to 344.7 mg C m<sup>-2</sup>·h<sup>-1</sup> (Table 2). Table 3 shows that CO<sub>2</sub> emissions from plots A to H increased in the order A < F < B < E < G < H < C < D, although the measured values for plots A, F, B, E, and G did not significantly differ from each other. Spatial variability of CO<sub>2</sub> emissions within individual plots was low, with coefficients of variation (CV) being 50%, 42%, 40%, 53%, 42%, 41%, 39%, and 15% for CO<sub>2</sub> fluxes for the A, B, C, D, E, F, G, and H plots, respectively. The average CO<sub>2</sub> emission flux of 579.7 mg CO<sub>2</sub> m<sup>-2</sup>·h<sup>-1</sup> from the *Artemisia scoparia* and *Pennisetum centrasiticum* plant

community (As+Pc type) (plots D, F, G, H) was lower than the value of 653.1 mg CO<sub>2</sub> m<sup>-2</sup>h<sup>-1</sup>, measured for the *Sophora alopecuroides* plant community (Sa type) (plot C), but the difference was not significant ( $P = 0.555$ ) (Fig. 3). The average CO<sub>2</sub> flux (307.2 mg CO<sub>2</sub> m<sup>-2</sup>h<sup>-1</sup>) from the *Peganum harmala* and *Stipa bungeana* plant community (Ph+Sb type) (plots A, B, E), however, was significantly lower than that from either the (As+Pc) or (Sa) type.

For all sampling plots, CO<sub>2</sub> emissions were positively and significantly correlated with soil pH ( $P < 0.05$ ) (Table 4, Fig. 4). The variation in soil pH at 0-10 cm depths could account for 53% of the spatial variation in CO<sub>2</sub> emissions across all investigated sites. The other soil properties, listed in Table 4, were not significantly correlated with spatial CO<sub>2</sub> emissions.

## Methane

Soils in the semiarid steppe of northern China act as a net sink for atmospheric CH<sub>4</sub>. Methane uptake by bare soils during the study period ranged from -67.4 to -6.9 μg C m<sup>-2</sup>h<sup>-1</sup>, while that by soils with plant cover ranged from -105.5 to -26.5 μg C m<sup>-2</sup>h<sup>-1</sup> (Table 2). The uptake of CH<sub>4</sub> by the eight plots increased in the order: A < D < E < H < G < C < F < B. (Table 3). In each plot, CH<sub>4</sub> uptake was highly variable, with a coefficient of variation (CV) ranging from -93.5% to -8%. The uptake of CH<sub>4</sub> by the (Ph+Sb) plant community type (-92.4±20.3 μg m<sup>-2</sup>h<sup>-1</sup>) tended to be higher than that by the (S) type (-84.3±16.5 μg m<sup>-2</sup>h<sup>-1</sup>) but the difference was not significant ( $P = 0.110$ ). However, the average CH<sub>4</sub> uptake (-67.5±27.8 μg m<sup>-2</sup>h<sup>-1</sup>)

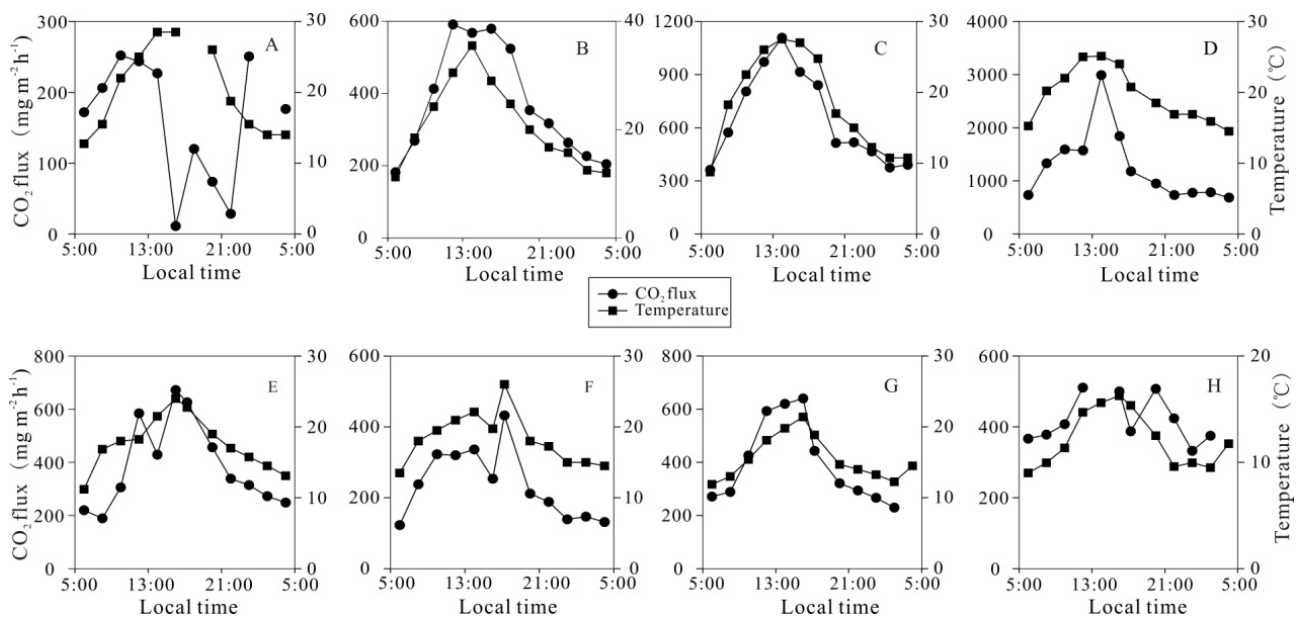


Fig. 2. Diurnal variations of CO<sub>2</sub> flux and air temperature in eight representative sites along the SIMWN transect. The symbols A to H refer to the sampling sites described in Table 1 and in the text.

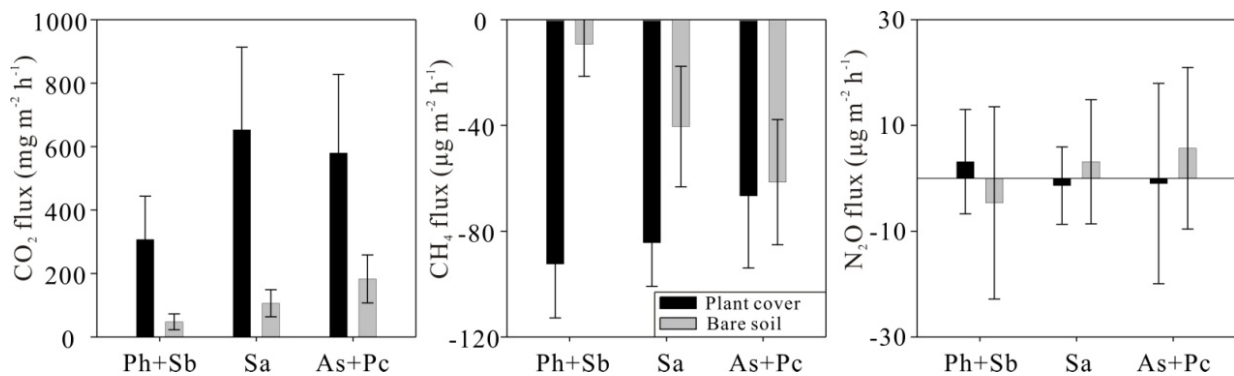


Fig. 3. Daily average CO<sub>2</sub>, CH<sub>4</sub>, and N<sub>2</sub>O fluxes from bare soils and from soils with plant cover along the SIMWN transect. The notations (Ph+Sb), (Sa), and (As+Pc) indicate plant communities dominated by *Peganum harmala* and *Stipa bungeana*, *Sophora alopecuroides*, *Artemisia scoparia*, and *Pennisetum centrasiatricum*, respectively. Plant communities (Ph+Sb), (Sa), and (As+Pc) are associated with sampling plots (A, B, E), (C), and (D, F, G, H), respectively. Error bars indicate standard deviation of fluxes among chambers.

Table 3. Mean fluxes of CO<sub>2</sub> (mg m<sup>-2</sup>·h<sup>-1</sup>), CH<sub>4</sub> (μg m<sup>-2</sup>·h<sup>-1</sup>), and N<sub>2</sub>O (μg m<sup>-2</sup>·h<sup>-1</sup>) and soil properties for eight sampling sites (A to H) along the SIMWN transect.

Site	CO <sub>2</sub> flux	CH <sub>4</sub> flux	N <sub>2</sub> O flux	AT (°C)	SW (%)	pH	NH <sub>4</sub> <sup>+</sup> -N (mg·kg <sup>-1</sup> )	SOC (g·kg <sup>-1</sup> )	TN (g·kg <sup>-1</sup> )
A	160.1d	-35.3a	0.98ab	20.7	1.9	7.91	12.4	9.8	0.54
B	373.8cd	-200.6e	-0.77ab	20.9	1.2	7.91	15.5	8.4	0.33
C	653.1b	-84.3d	-1.38ab	18.9	4.3	8.36	1.6	11.0	0.52
D	1264.0a	-40.1ab	-4.80b	19.6	2.0	8.24	12.4	9.2	0.43
E	387.9cd	-41.4ab	9.21a	17.7	10.6	7.95	7.0	27.9	0.67
F	236.9cd	-94.6d	-1.16ab	18.3	5.9	7.88	8.1	16.9	0.59
G	399.1cd	-76.7cd	1.04ab	15.6	13.1	7.98	8.7	19.5	0.51
H	418.7bc	-58.5bc	1.09ab	12.1	18.3	7.94	19.8	24.6	0.57

The symbols A to H refer to the sampling sites (plots) as described in Table 1 and in the text.

AT – air temperature; SW – soil water content (0-10 cm depth).

Letters in superscript indicate a significant difference among sites at the 5% level ( $P < 0.05$ ).

Table 4. Correlation coefficients of GHG fluxes against air temperature and some soil/plant factors.

	CO <sub>2</sub> flux	CH <sub>4</sub> flux	N <sub>2</sub> O flux
CO <sub>2</sub> flux	1	0.084	-0.545
CH <sub>4</sub> flux	0.084	1	0.374
N <sub>2</sub> O flux	-0.545	0.374	1
Air temperature	0.114	-0.336	-0.231
Soil water content	-0.237	0.347	0.423
Soil pH	0.728*	0.226	-0.410
Soil NH <sub>4</sub> <sup>+</sup> -N	0.141	-0.282	-0.374
Soil organic C	-0.352	0.415	0.752*
Soil total N	-0.464	0.717*	0.781*
Soil C/N	-0.259	0.175	0.586
Plant total C	0.337	-0.095	-0.592
Plant total N	0.105	-0.387	-0.305
Plant C/N	-0.071	0.493	0.381

\*indicates the significance level  $P < 0.05$ .

by the (As+Pc) plant community type was significantly lower than that by the (Ph+Sb) type ( $P = 0.000$ ) or the (Sa) type ( $P = 0.010$ ) (Fig. 3).

Stepwise linear regression analysis indicated that only soil total nitrogen (TN) had a significant influence on the spatial variability of CH<sub>4</sub> flux in the grasslands across the transect. TN could explain 51% of the spatial variance in CH<sub>4</sub> uptake ( $P < 0.05$ ) (Table 4; Fig. 5). In other words, soil temperature, soil pH, soil organic carbon (SOC), C/N ratio, and C and N contents of plant tissues (Table 4) do not appear to be significantly related to spatial CH<sub>4</sub> flux.

## Nitrous Oxide

The flux of N<sub>2</sub>O (uptake and emission) for the bare soils at all eight sites ranged from -2.9 to 6.1 μg N m<sup>-2</sup>·h<sup>-1</sup>, which was comparable to the range measured for the soils with plant cover (-3.1 to 5.9 μg N m<sup>-2</sup>·h<sup>-1</sup>) (Table 2). However, the mean N<sub>2</sub>O emissions from the bare soils (2.2±9.7 μg N m<sup>-2</sup>·h<sup>-1</sup>) was much higher than that from the plant-covered counterparts (0.3±8.8 μg N m<sup>-2</sup>·h<sup>-1</sup>). Statistical analysis indicated a significant difference in N<sub>2</sub>O flux between plot D and plot E ( $P = 0.031$ ), but the values measured for the other six plots were not significantly different (Table 3). Like that for methane, the coefficient of variance (CV) for the N<sub>2</sub>O flux, ranging from -13.9 to 23.5%, showed a high heterogeneity among sampling plots. The mean N<sub>2</sub>O uptake by the (Sa) plant community type of

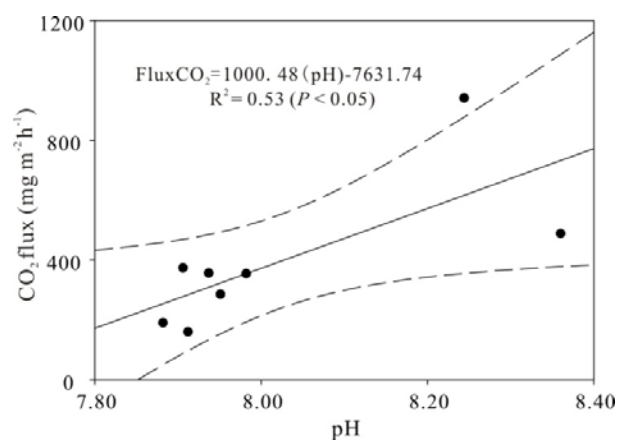


Fig. 4. Correlation of CO<sub>2</sub> emission rates corrected by vegetation coverage with surface soil pH for the eight sites (A to H) along the SIMWN transect. The solid lines were fitted by linear regression, the dotted lines represent the 95% confidence intervals.

Table 5. Comparison of the cumulative CO<sub>2</sub>, CH<sub>4</sub>, and N<sub>2</sub>O fluxes and their global warming potentials (GWPs) (expressed in CO<sub>2</sub>-equivalent) between the pastoral area and the agro-pastoral ecotone.

Land use	Vegetation	Area (ha)	CO <sub>2</sub> flux		CH <sub>4</sub> flux		N <sub>2</sub> O flux	
			A	B	A	B	A	B
Pastoral area	Bare soil	831,000	8028.4	29437.3	-7.4	-245.8	0.44	208.0
	Plant cover	1,939,000	61770.2	226390.7	-27.6	-919.1	0.15	69.3
Agro-pastoral ecotone	Bare soil	744,000	7187.9	26355.5	-6.6	-220.1	0.40	186.2
	Plant cover	1,736,000	55303.3	202778.7	-24.7	-822.9	0.13	62.1

A – cumulative GHG fluxes (t CO<sub>2</sub>-C d<sup>-1</sup>, t CH<sub>4</sub>-C d<sup>-1</sup>, and t N<sub>2</sub>O-N d<sup>-1</sup>, respectively), B – cumulative GWP (t C-eq·d<sup>-1</sup>)

1.4±7.3 μg m<sup>-2</sup>·h<sup>-1</sup> was higher than that by (As+Pc) type (1.0±18.5 μg m<sup>-2</sup>·h<sup>-1</sup>), but the difference was not significant (P>0.05) (Fig. 3).

The average N<sub>2</sub>O flux for all sites was positively and significantly correlated with both SOC and TN (Table 4, Fig. 6), with SOC accounting for 57% of the spatial variation in

N<sub>2</sub>O emissions (P < 0.05). Thus, a multiple linear regression model incorporating both SOC and TN led to a significant improvement in explaining the variability in N<sub>2</sub>O emissions (R<sup>2</sup> = 0.67). The other soil factors in Table 4 did not appear to have a significant effect on N<sub>2</sub>O fluxes.

## Discussion

### Regional Greenhouse gas Fluxes and Global Warming Potential

The daily average fluxes of GHG for the bare soils along the SIMWN transect were 40.3±16.8 mg CO<sub>2</sub>-C m<sup>-2</sup>·h<sup>-1</sup>, -37.0±16.2 μg CH<sub>4</sub>-C m<sup>-2</sup>·h<sup>-1</sup>, and 2.2±9.7 μg N<sub>2</sub>O-N m<sup>-2</sup>·h<sup>-1</sup>, while the values for the soils with plant cover were 132.7±56.6 mg CO<sub>2</sub>-C m<sup>-2</sup>·h<sup>-1</sup>, -59.3±17.7 μg CH<sub>4</sub>-C m<sup>-2</sup>·h<sup>-1</sup>, and 0.3±8.8 μg N<sub>2</sub>O-N m<sup>-2</sup>·h<sup>-1</sup> (Table 2). In the semiarid steppe of northern China, the pastoral area covers 2.77×10<sup>6</sup> ha and the agro-pastoral ecotone amounts to 2.48×10<sup>6</sup> ha [19]. Assuming that our measurements are representative of regional GHG fluxes, and that 70% of the sites had a plant cover while 30% were bare during summer [20, 21], the cumulative GHG fluxes amounted to 7.0×10<sup>4</sup> t CO<sub>2</sub>-C, -35.0 t CH<sub>4</sub>-C, and 0.6 t N<sub>2</sub>O-N per day for the pastoral

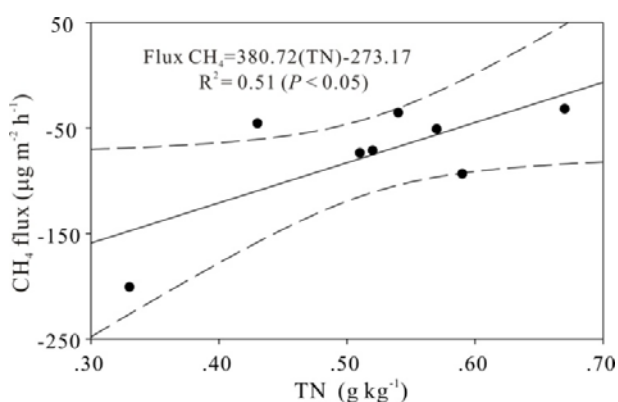


Fig. 5. Correlation of CH<sub>4</sub> flux rates corrected by vegetation coverage with soil total nitrogen (TN) for the eight sites (A to H) along the SIMWN transect. The solid lines were fitted by linear regression, the dotted lines represent the 95% confidence intervals.

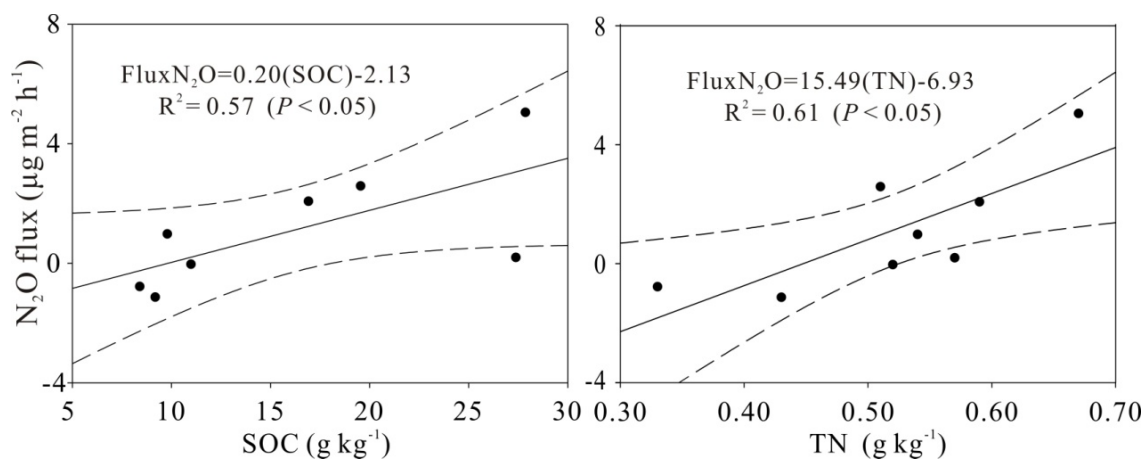


Fig. 6. Correlation of N<sub>2</sub>O flux rates corrected by vegetation coverage with soil organic carbon (SOC) and soil total nitrogen (TN) for the eight sites (A to H) along the SIMWN transect. The solid lines were fitted by linear regression, the dotted lines represent the 95% confidence intervals.

area, while the corresponding values for the agro-pastoral ecotone were  $6.2 \times 10^4$  t CO<sub>2</sub>-C, -31.3 t CH<sub>4</sub>-C, and 0.5 t N<sub>2</sub>O-N per day (Table 5).

The daily average flux in CO<sub>2</sub> equivalents is estimated for each GHG based on global warming potentials (GWP). According to equation (1), the GWP from the pastoral area during the measurement period ( $8.9 \times 10^2$  t C-eq) is larger than that from the agro-pastoral ecotone ( $7.9 \times 10^2$  t C-eq). Thus, in terms of GWP the pastoral area exerts a greater mitigation effect than the agro-pastoral ecotone if only CH<sub>4</sub> and N<sub>2</sub>O are considered (Table 5). When the emission of CO<sub>2</sub> is taken into account, however, the contribution of the pastoral area to the regional GWP ( $2.6 \times 10^5$  t C-eq·d<sup>-1</sup>) during the measurement period is larger than that of the agro-pastoral ecotone ( $2.3 \times 10^5$  t C-eq·d<sup>-1</sup>) (Table 5). As we did not consider the landscape (topography, soil texture) and seasonal amplitudes of GHG fluxes, the above estimate does not necessarily represent annual GWP, although it provides insight into the relative contribution of CO<sub>2</sub>, CH<sub>4</sub>, and N<sub>2</sub>O to the GHG budget in the region investigated. Given its huge extent, however, the semiarid steppe in northern China would be expected to act as a net carbon source, at least in midsummer.

#### Effect of Vegetative Cover and Type on GHG Fluxes

Vegetation could affect ecosystem respiration by influencing plant community microclimate and structure, the quantity and quality of detritus supplied to the soil, and the overall rate of plant and soil respiration. Regardless of location along the transect, CO<sub>2</sub> emissions were significantly higher from soils with plant cover than that from bare soils ( $P = 0.023$ ) (Table 2, Fig. 3). This finding is consistent with the suggestion that the rhizosphere of plant-covered soils is the site of high microbial activity [22, 23], and that most of the root respiration stems from recently fixed carbon associated with above-ground plant growth and below-ground root growth [24]. Assuming that plant respiration ( $R_{\text{plant}}$ ) equals ecosystem (plant community) respiration ( $R_{\text{eco}}$ ) minus bare soil respiration ( $R_{\text{soil}}$ ), we estimate that the contribution of  $R_{\text{plant}}$  to  $R_{\text{eco}}$  for the plant community types (Ph+Sb), (Sa), and (As+Pc) during the measurement period was 84.5, 83.7, and 68.5%, respectively (Fig. 3). These percentages are consistent with the range of values reported by other investigators [25, 26].

In agreement with Schimel [27], more CH<sub>4</sub> was taken up by soils with vegetative cover (canopy) along the transect than by the corresponding bare soils (Table 2, Fig. 3). This finding indicates that the plant canopy acts as a physical barrier to CH<sub>4</sub> diffusion (from soil to atmosphere). The presence of plant cover also enhances the probability that CH<sub>4</sub> would be oxidized before being emitted to the atmosphere, as rhizospheric oxidation may contribute more than 80% to total oxidation in soil-plant systems [4]. Since such constraints do not apply to bare soils, relatively less methane was taken up in the absence of plant cover.

Further, the oxygen released into the rhizosphere (by plant roots) would be consumed by methane-oxidizing bacteria, as a result of which methanogenesis is inhibited [28].

Several studies [29-31] have indicated that plants can contribute appreciably to the emission of N<sub>2</sub>O from soil-plant systems. The N<sub>2</sub>O emitted from above-ground plant biomass may comprise a mixture of phytogenic N<sub>2</sub>O and N<sub>2</sub>O produced by soil microorganisms but transported by plants [32]. Our results, however, suggest that different plant community types have different effects on N<sub>2</sub>O emission (Fig. 3). But in general, the plant exerts a constraining influence on cumulative N<sub>2</sub>O fluxes from the whole of semiarid steppe, which is in agreement with other studies [33, 34]. The flux of N<sub>2</sub>O increased in the presence of plants, particularly when soil moisture was relatively high, and when soil temperature exceeded 19°C [35]. Under such conditions, the parenchymal system can actively transport oxygen from shoots to roots as well as gases from soil to atmosphere [34], whereas N<sub>2</sub>O is largely emitted from soil to atmosphere when soil moisture is low [33].

As all of our sampling plots are located in the semiarid region, soil gravimetric water content was low (1.2-18.3% w/w, while nearly 2/3 of the grassland sites contain less than 6% w/w moisture) (Table 3). Under these conditions, N<sub>2</sub>O is consumed by the plant community, as Donoso et al. [36] and Li et al. [37] have previously reported. Secondly, plants alter the community structure of soil microorganisms, and denitrification in the rhizosphere is enhanced by the increase in carbon stock from root decomposition. As a result, consumption of N<sub>2</sub>O increases, as does N<sub>2</sub> formation through denitrification [32].

#### Environmental Factors Influencing GHG Fluxes

In the steppe of northern China, air temperature and relative humidity were the main factors regulating the diurnal variation of CO<sub>2</sub> fluxes (Fig. 2) except for plot A, where some rain fell during the night of measurement. Precipitation strongly stimulates soil CO<sub>2</sub> fluxes in surface layers where biological activity is concentrated by a “drying and rewetting effect” [38]. Similarly, CO<sub>2</sub> emissions increase with a rise in temperature. This effect is associated with an increase in root respiration and microbially induced mineralization of soil organic matter [39]. Diurnal variations in temperature, and their effect on CO<sub>2</sub> emissions, should therefore be considered in modeling CO<sub>2</sub> sources and sinks [40]. We might also add that global warming would increase CO<sub>2</sub> emissions from soils and accelerate the depletion of SOC.

The pH of surface soils and its variation between single measurement points at each site showed a significant positive correlation with CO<sub>2</sub> emissions (Table 4, Fig. 4) in accord with previous results for other soil types [41, 42]. CO<sub>2</sub> emissions increased with soil pH, presumably because of its positive effect of pH on the growth and proliferation of soil microbes.



No significant correlation ( $P < 0.05$ ) was found between SOC and CH<sub>4</sub> fluxes with Pearson's coefficient being 0.415 in general (Table 4). A significant negative relationship, however, was observed between TN and spatial CH<sub>4</sub> fluxes for the semiarid steppe in northern China (Fig. 5), suggesting that the higher the TN the lower the uptake of atmospheric CH<sub>4</sub> by soil. A similar relationship has been reported for forest soils [43], agricultural soils [44], and grassland soils [45].

Previous studies [46, 47] have shown that the concentration of N<sub>2</sub>O in various soils, derived from nitrification and denitrification, is positively correlated with SOC and TN. Thus, soils with high SOC and TN contents generally show high N<sub>2</sub>O fluxes. We have found similarly for the semiarid grasslands in northern China in that the relationship of N<sub>2</sub>O flux with SOC and TN had correlation coefficients of 0.752 ( $P = 0.031$ ) and 0.781 ( $P = 0.022$ ), respectively (Table 4, Fig. 6). Since for many surface soils SOC is proportional to TN, the relationship between N<sub>2</sub>O flux and SOC is very similar to that between N<sub>2</sub>O flux and TN. Our measurements indicate that soil organic matter is very important in determining the magnitude of the spatial N<sub>2</sub>O flux, at least in the semiarid steppe.

### Acknowledgements

This research was supported by the National Natural Science Foundation of China (Nos. 40872212, 41021062, 41103078), the Strategic Priority Research Program of the Chinese Academy of Sciences (XDA05070400), National Key Basic Research Project of China (2013CB956700-2); the Key Agriculture R&D Program of Guizhou Province (Qian Science co-NY [2011] No. 3079, Qian Science co-NY [2013] No. 3019), and the Natural Science Foundation of Guizhou Province (Qian Science co-J [2011] No. 2054).

### References

1. BALEZENTIENE L., BLEIZGYS R. Short-term inventory of GHG fluxes in semi-natural and anthropogenized grassland. *Pol. J. Environ. Stud.* **20**, 255, **2011**.
2. BALEZENTIENE L., UZUPIS A. Multi-criteria optimization for mitigation model of greenhouse gas emissions from abandoned grassland. *J. Food Agr. Environ.* **10**, 859, **2012**.
3. AMBUS P., CHRISTENSEN S. Measurement of N<sub>2</sub>O emission from a fertilized grassland: an analysis of spatial variability. *J. Geophys. Res.* **99**, 16549, **1994**.
4. VAN DEN POL-VAN DASSELAAR A., CORRE W. J., PRIEME A., KLEMEDTSSON A. K., WESLIEN, P., STEIN A., KLEMEDTSSON L., OENEMA O. Spatial variability of methane, nitrous oxide, and carbon dioxide emissions from drained grasslands. *Soil Sci. Soc. Am. J.* **62**, 810, **1998**.
5. YAO Z. S., WOLF B., CHEN W. W., BUTTERBACH-BAHL K., BRUGGEMANN N., WIESMEIER M., DANNENMANN M., BLANK B., ZHENG X. H. Spatial variability of N<sub>2</sub>O, CH<sub>4</sub> and CO<sub>2</sub> fluxes within the Xilin River catchment of Inner Mongolia, China: a soil core study. *Plant Soil.* **331**, 341, **2010**.
6. KATO T., HIROTA M., TANG Y. H., WADA E. Spatial variability of CH<sub>4</sub> and N<sub>2</sub>O fluxes in alpine ecosystems on the Qinghai-Tibetan Plateau. *Atmos. Environ.* **45**, 5632, **2011**.
7. TIESZEN L. L., DETLING J. Productivity of grassland and tundra. In: LANGE O. L. NOBEL P. S., OSMOND C. G., ZIEGLER H. (Eds.), *Physiological Plant Ecology IV. Ecosystem Processes: Mineral Cycling, Productivity and Man's Influence*. Encyclopedia of Plant Physiology. Springer-Verlag, Berlin, **1983**.
8. ANDERSON J. M. The effects of climate change on decomposition processes in grassland and coniferous forests. *Ecol. Appl.* **1**, 326, **1991**.
9. ESWARAN H., VANDENBERG E., REICH P. Organic carbon in soils of the world. *Soil Sci. Soc. Am. J.* **57**, 192, **1993**.
10. CHEN Z. Z., WANG S. P. Typical grassland ecosystem in China. Science Press, Beijing, **2000** [In Chinese].
11. ZHAO W. L., QI J. G., SU G. J., LI F. M. Spatial patterns of top soil carbon sensitivity to climate variables in northern Chinese grasslands. *Acta Agr. Scand. B-S P.* **62**, 720, **2012**.
12. STOYAN H., DE-POLLI H., BOHM S., ROBERTSON G.P., PAUL E.A. Spatial heterogeneity of soil respiration and related properties at the plant scale. *Plant Soil.* **222**, 203, **2000**.
13. FOLORUNSO O.A., ROLSTON D.E. Spatial variability of field-measured denitrification gas fluxes. *Soil Sci. Soc. Am. J.* **48**, 1214, **1984**.
14. WANG Y. S., XUE M., ZHENG X. H., JI B. M., DU R., WANG Y. F. Effects of environmental factors on N<sub>2</sub>O emission from and CH<sub>4</sub> uptake by the typical grasslands in the Inner Mongolia. *Chemosphere.* **58**, 205, **2005**.
15. LIU X. R., DONG Y. S., QI Y. C., LI S. G. N<sub>2</sub>O fluxes from the native and grazed semi-arid steppes and their driving factors in Inner Mongolia, China. *Nutr. Cycl. Agroecos.* **86**, 231, **2010**.
16. DU R., LU D., WANG G. Diurnal, seasonal, and inter-annual variations of N<sub>2</sub>O fluxes from native semiarid grassland soils of inner Mongolia. *Soil Biol. Biochem.* **38**, 3474, **2006**.
17. WANG Y. S., WANG Y. H. Quick measurement of CH<sub>4</sub>, CO<sub>2</sub> and N<sub>2</sub>O emissions from a short-plant ecosystem. *Adv. Atmos. Sci.* **20**, 842, **2003**.
18. FORSTER P., RAMASWAMY V., ARAXO P., BERNTSEN T., BETTS R. A., FAHEY D. W., HAYWOOD J., LEAN J., LOWE D. C., MYHRE G., NGANGA J., PRINN R., RAGA G., SCHULZE M., VAN DORLAND R. Changes in atmospheric constituents and in radiative forcing. In: SOLOMON S., QIN D., MANNING M., CHEN Z., MARQUIS M., AVERYT K.B., TIGNOR M. MILLER H.L. (Eds), *Climate Change 2007: The Physical Science Basis. Contribution of Working Group I to the Fourth Assessment Report of the Intergovernmental Panel on Climate Change*, Cambridge University Press, New York, **2007**.
19. YAN C. Z., WANG Y. M., FENG Y. S., WANG J. H., WU W. Macro-scale study on grassland cover of Ningxia region by remote sensing in the digital way. *J. Desert Res.* **20**, 298, **2000** [In Chinese].
20. SU Y. Z., LI Y. L., ZHAO H. L. Soil properties and their spatial pattern in a degraded sandy grassland under post-grazing restoration, Inner Mongolia, northern China. *Biogeochemistry.* **79**, 297, **2006**.
21. FU C. B., JIANG Z. H., GUAN Z. Y., HE J. H., XU Z. F. *Regional climate studies of China*. Springer-Verlag Berlin Heidelberg, **2008**.

22. RAICH J. W., TUFEKCIOGLU A. Vegetation and soil respiration: Correlations and controls. *Biogeochemistry*. **48**, 71, **2000**.
23. STEER J., HARRIS J. A. Shifts in the microbial community in rhizosphere and non-rhizosphere soils during the growth of *Agrostis stolonifera*. *Soil Biol. Biochem.* **32**, 869, **2000**.
24. MARINIER M., GLATZEL S., MOORE T. R. The role of cotton-grass (*Eriophorum vaginatum*) in the exchange of CO<sub>2</sub> and CH<sub>4</sub> at two restored peatlands, eastern Canada. *Ecoscience*. **11**, 141, **2004**.
25. WANG G. C., DU R., KONG Q. X., LU D. R. Experimental study on soil respiration of temperate grassland in China. *Chinese Sci. Bull.* **49**, 642, **2004**.
26. WANG W., GUO J. X., FENG J., OIKAWA T. Contribution of root respiration to total soil respiration in a *Leymus chinensis* (Trin.) Tzvel. grassland of northeast China. *J. Integr. Plant Biol.* **48**, 409, **2006**.
27. SCHIMMEL J. P. Plant transport and methane production as controls on methane flux from Arctic wet meadow tundra. *Biogeochemistry*. **28**, 183, **1995**.
28. LAANBROEK H. J. Methane emission from natural wetlands: interplay between emergent macrophytes and soil microbial processes. A mini-review. *Ann. Bot.* **105**, 141, **2010**.
29. HAKATA M., TAKAHASHI M., ZUMFT W., SAKAMOTO A., MORIKAWA H. Conversion of the nitrate nitrogen and nitrogen dioxide to nitrous oxides in plants. *Acta Biotechnol.* **23**, 249, **2003**.
30. MULLER C. Plants affect the *in situ* N<sub>2</sub>O emissions of a temperate grassland ecosystem. *J. Plant Nutr. Soil Sc.* **166**, 771, **2003**.
31. PIHLATIE M., AMBUS P., RINNE J., PILEGAARD K., VESALA T. Plant-mediated nitrous oxide emissions from beech (*Fagus sylvatica*) leaves. *New. Phytol.* **168**, 93, **2005**.
32. DU Y. G., CAO G. M., DENG Y. C., SUN G. C., CUI X. Y. Contribution of the vegetation layers in the nitrous oxide emission from Alpine *Kobresia humilis* SERG. meadow ecosystem on the Tibetan plateau. *Pol. J. Ecol.* **58**, 115, **2010**.
33. YAN X., SHI S., DU L., XING G. Pathways of N<sub>2</sub>O emission from rice paddy soil. *Soil Biol. Biochem.* **32**, 437, **2000**.
34. HERNANDEZ M. E., MITSCH W. J. Influence of hydrologic pulses, flooding frequency, and vegetation on nitrous oxide emissions from created riparian marshes. *Wetlands*. **26**, 862, **2006**.
35. UCHIDA Y. The effects of substrate, temperature and soil fertility on respiration and N<sub>2</sub>O production in pastoral soils. Ph thesis, Lincoln University, New Zealand, **2010**.
36. DONOSO L., SANTANA R., SANHUEZA E. Seasonal variation of N<sub>2</sub>O fluxes at a tropical savannah site: soil consumption of N<sub>2</sub>O during the dry season. *Geophys. Res. Lett.* **20**, 1379, **1993**.
37. LI J., LEE X., YU Q., TONG X., QIN Z., MACDONALD B. Contributions of agricultural plants and soils to N<sub>2</sub>O emission in a farmland. *Biogeosciences*. **8**, 5505, **2011**.
38. LEE M. S., NAKANE K., NAKATSUBO T., MO W. H., KOIZUMI H. Effects of rainfall events on soil CO<sub>2</sub> flux in a cool temperate deciduous broad-leaved forest. *Ecol. Res.* **17**, 401, **2002**.
39. LA SCALA JR N., SIMAS F. N. B., DE SA MENDONCA E., SOUZA J. V., PANOSSO A. R., SCHAEFER C. E. G. R. Spatial and temporal variability of soil C-CO<sub>2</sub> emissions and its relation with soil temperature in King George Island, Maritime Antarctica, 19<sup>th</sup> World Congress of Soil Science, Soil Solutions for a Changing World, Brisbane, Australia. Published on DVD, **2010**.
40. DONG Y. S., ZHANG S., QI Y. C., CHEN Z. Z., GENG Y. B. Fluxes of CO<sub>2</sub>, N<sub>2</sub>O and CH<sub>4</sub> from a typical temperate grassland in Inner Mongolia and its daily variation. *Chinese Sci. Bull.* **45**, 1590, **2000**.
41. CABANEIRO A., FERNANDEZ I., PEREZ-VENTURA L., CARBALLAS T. Soil CO<sub>2</sub> emissions from Northern Andean Paramo ecosystems: Effects of fallow agriculture. *Environ. Sci. Technol.* **42**, 1408, **2008**.
42. SETIA R., MARSCHNER P., BALDOCK J., CHITTLEBOROUGH D., VERMA V. Relationships between carbon dioxide emission and soil properties in salt-affected landscapes. *Soil Biol. Biochem.* **43**, 667, **2011**.
43. ROSENKRANZ P., BRUGGEMANN N., PAPAN H., XU Z., HORVATH L., BUTTERBACH-BAHL K. Soil N and C trace gas fluxes and microbial soil N turnover in a sessile oak (*Quercus petraea* (Matt.) Liebl.) forest in Hungary. *Plant Soil*. **286**, 301, **2006**.
44. SITAULA B. K., HANSEN S., SITAULA J. I. B., BAKKEN L. R. Methane oxidation potentials and fluxes in agricultural soil: Effects of fertilisation and soil compaction. *Biogeochemistry*. **48**, 323, **2000**.
45. MOSIER A., SCHIMMEL D., VALENTINE D., BRONSON K., PARTON W. Methane and nitrous oxide fluxes in native, fertilized and cultivated grasslands. *Nature*. **350**, 330, **1991**.
46. VINTHER F. P. Measured and simulated denitrification activity in a cropped sandy and loamy soil. *Biol. Fert. Soils*. **14**, 43, **1992**.
47. PAPAN H., BUTTERBACH-BAHL K. A 3-year continuous record of nitrogen trace gas fluxes from untreated and limed soil of a N-saturated spruce and beech forest ecosystem in Germany – 1. N<sub>2</sub>O emissions. *J. Geophys. Res.* **104**, 18487, **1999**.